Journal of proteome research

Article

Cite This: J. Proteome Res. 2018, 17, 3932−3940

pubs.acs.org/jpr

Multiplex Immuno-Liquid Chromatography−Mass Spectrometry−Parallel Reaction Monitoring (LC−MS−PRM) Quantitation of CD8A, CD4, LAG3, PD1, PD-L1, and PD-L2 in Frozen Human Tissues

Qian Zhang, Robert Salzler, Anthony Dore, Janice Yang, Dangshe Ma, William C. Olson, and Yashu Liu*

Regeneron Pharmaceuticals, 777 Old Saw Mill River Road, Tarrytown, New York 10591, United States

Supporting Information

ABSTRACT: The immune status of tumors critically influences their responsiveness to PD1 blockades and other immune-based therapies. Programmed death ligand 1 (PD-L1) immunohistochemistry (IHC) is a clinically validated predictive biomarker of response to checkpoint-inhibitor therapy in a limited number of clinical settings but is poorly predictive in most. With emerging evidence that multiple pathways and immune-checkpoint proteins may coordinately contribute to the adaptive immune resistance, the identification and quantitation of multiple immune markers in tumor tissue could help identify the controlling pathways in a given patient, guide the selection of optimal therapy, and monitor response to treatment. We developed and validated a sensitive and robust immuno-liquid chromatography−parallel reaction monitoring assay to simultaneously quantify the expression levels of six immune markers (CD8A, CD4, LAG3, PD1, PD-L1, and PD-L2) using as little as 1−2 mg of fresh frozen tissue. The lower limit of quantitation ranged from 0.07 ng/mg protein for PD1 to 1.0 ng/mg protein for CD4. The intrabatch accuracy was within −16.6% to 15.0% for all proteins at all concentrations, and the variation ranged from 0.8% to 14.7%, while interbatch accuracy was within −6.3% to 8.6%, and the variation ranged from 1.3% to 12.8%. The validated assay was then applied to quantify all six biomarkers in different tissues and was confirmed to have sufficient sensitivity (0.07−1.00 ng/mg protein) and reproducibility (variation ranged from 4.3 to 12.0%). In an analysis of 26 cervical tumors, CD8A and CD4 were detected in all tumors, followed by PD-L1 in 85%, LAG-3 in 65%, PD1 in 50%, and PD-L2 in 35%. The strongest correlations were observed between CD8A and CD4 (r = 0.88) and CD8A and LAG-3 (r = 0.86). PD1 was not significantly correlated with any of the other proteins tested. This method can be applied to survey the immune signatures across tumor types and tailored to incorporate additional markers as needed.

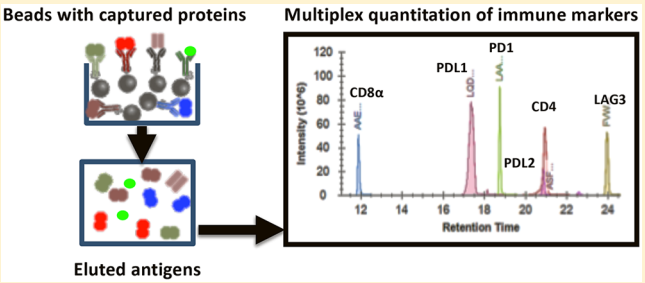

KEYWORDS: *tumor-infiltrating lymphocytes, immuno-oncology, PD1, PD-L1, PD-L2, LAG3, CD4, CD8, PRM quantitation, assay validation*

INTRODUCTION

T cells and other immune effector cells can infiltrate and eliminate tumors but often get repressed via suppressive mechanisms within the tumor microenvironment.[1−3] Antibodies to PD1 and other checkpoint molecules can reinvigorate T cells and provide unprecedented clinical benefit in some patients.[4−8] However, sustained tumor regressions are observed in varying fractions of patients across different tumor types, and there is intense interest in identifying the correlates of response and resistance to checkpoint inhibitor therapy. Immunohistochemistry (IHC) of PD-L1 expression is a predictive biomarker of response to therapy with anti-PD1 and anti-PD-L1 antibodies in non-small cell lung, bladder, and cervical cancers but not in other cancers, in which these agents are approved for use. PD-L1 IHC is limited by its subjective nature and the differing clones and cut-offs used in different settings. In addition, several pathways regulate T-cell suppression and activation in tumors, suggesting that combinations of immune-based therapies and multiplex biomarker assays may be required for optimal therapy in most patients.

Parallel reaction monitoring (PRM)- and multiple reaction monitoring (MRM)-based mass spectrometry (MS) have proven to be highly specific and robust platforms for accurate protein quantitation from diverse biological matrices. A desired sensitivity can be reached when combining MRM and PRM quantitation with various protein- and peptide-enrichment steps. MRM and PRM assays have been routinely used for preclinical pharmacokinetics analysis of monoclonal antibodies[9] and have been validated to evaluate plasma levels of nerve growth factor (NGF) in patients receiving anti-NGF therapy.[10]

Received: August 6, 2018
Published: October 2, 2018

DOI: 10.1021/acs.jproteome.8b00605
J. Proteome Res. 2018, 17, 3932−3940

Table 1. PRM Parameters of Monitored Peptides and SILs

protein	MW (kDa)	monitored peptide	parent m/z	fragment m/z	HCD energy	LLOQ (ng/mg total protein)
CD4	51.1	ILGNQGSFLTK	589.33	780.43 (y7), 652.37 (y6)	23	1.00
			593.34	788.44 (y7), 660.38 (y6)		
CD8a	25.7	AAEGLDTQR	480.74	818.40 (y7), 689.36 (y6)	23	0.95
			485.75	828.41 (y7), 699.37 (y6)		
LAG3	57.4	FVWSSLDTPSQR	711.85	990.48 (y9), 588.31 (y5)	23	0.15
			716.86	1000.49 (y9), 598.32 (y5)		
PD1	31.6	LAAFPEDR	459.74	663.31 (y5), 516.24 (y4)	23	0.07
			464.74	673.32 (y5), 526.25 (y4)		
PD-L1	33.3	LQDAGVYR	461.24	680.34 (y6), 494.27 (y4)	23	0.25
			466.25	690.34 (y6), 504.28 (y4)		
PD-L2	31.0	ASFHIPQVQVR	427.91	726.43 (y6), 501.31 (y4)	27	0.25
			431.24	736.43 (y6), 511.32 (y4)		

As for tissue samples, Kennedy et al. developed a SISCAPA-based MRM assay to quantify multiple proteins from frozen and FFPE tissues[11] using antibodies custom generated against the specific tryptic peptides. Antibody-independent protein quantitation can also be achieved through an additional dimension of liquid chromatography (LC) separation, such as strong cation exchange (SCX)[12] or basic reverse-phase (bRP),[13] to enrich the targeted peptide in an off-line mode. Fractions containing the targeted peptides are then collected and reinjected onto online LC coupled with mass spectrometry. Compared with IHC methods, MS-based quantitation is typically more sensitive, more quantitative, and less subjective in analyzing a given target.[14,15]

Here, we describe a novel PRM-based assay that uses automated affinity enrichment coupled with nano-LC-PRM quantitation to simultaneously evaluate the expression of six immune markers (CD8A, CD4, LAG3, PD1, PD-L1, PD-L2) from frozen cancerous and normal tissues. The assay was designed in a 96-well plate format and validated to enable the accurate and robust analysis of clinical samples. Analytes are measured simultaneously in a single process run, facilitating quantitative comparisons among the markers and minimizing sample requirements. In an initial study, the assay was sensitive enough to measure the absolute concentration of these markers in different tissues, including a panel of 26 cervical tumors. This report describes the performance characteristics of the method along with the absolute levels and correlations among the markers across an initial panel of tissues analyzed.

MATERIAL AND METHODS

Reagents

Recombinant human sCD4, LAG3.Fc, PD1.Fc, PD-L1.Fc, and PD-L2.Fc proteins were purchased from R&D systems, and recombinant human CD8A ectodomain protein with a carboxy-terminal myc-myc-hexahistidine (mmH) tag was prepared in-house. Biotinylated anti-hCD4 (OKT4), anti-hLAG3 (clone no. 11C3C65), anti-hPD1 (clone no. NAT105), anti-hPD-L1 (clone no. 29E.2A3), and anti-hPD-L2 (clone MIH18) were obtained from Biolegend, and biotinylated anti-hCD8A (OKT8) was purchased from Invitrogen. The stable-isotope-labeled (SIL) peptides (Tables 1 and S13) were synthesized by New England Peptides with 98% purity using high-performance liquid chromatography (HPLC) by the vendor, and the amino acid sequences were further confirmed in house using a Q Exactive Plus mass spectrometer (Thermo Fisher). The lysis buffer, protease inhibitor, 96-well plates, and all buffers and solvents were purchased from Thermo Scientific. Urea and iodoacetamide were obtained from Sigma-Aldrich. Trypsin and Lys-C were purchased from Promega Biosciences. Liver tissues from C57BL/6 mice were collected in-house, and all fresh frozen human tissue samples (Table S12) were acquired from ProteoGenex Inc.

Preparation of Tissue Lysate, Calibration, and QC Standards

Each fresh frozen tissue was weighed and powdered in liquid nitrogen. The powders were lysed with prechilled lysis buffer (0.1 M Tris pH 8.0, 1% NP-40, 1× protease inhibitor). Proteins were extracted by incubating the lysate on ice for 30 min with sonication for 30 s every 10 min. The lysate was then centrifuged for 30 min at 40000*g*. The total protein concentration in the supernatant was measured using BCA protein quantitation kit. Each sample was then aliquoted and stored at −80 °C prior to use.

All lysates from mouse livers were pooled to use as the surrogate matrix for the calibration standards and QC samples. Recombinant CD8a.mmh, sCD4, LAG3.Fc, PD1.Fc, PD-L1.Fc, and PD-L2.Fc were spiked into mouse liver lysate at a final concentration ranging from 0.09 to 200 ng/mg protein (1:2 serial dilution). QC standards were prepared in the same manner with 1.5 ng/mg as for LQC, 15 ng/mg as for MQC, and 150 ng/mg as for HQC. QC standards were aliquoted and stored at −80 °C, and calibration standards were prepared freshly for individual experiment.

Target Enrichment and Digestion

A total of 500 μg of biotinylated anti-CD8A, anti-CD4, anti-LAG3, anti-PD1, anti-PD-L1, and anti-PD-L2 were separately incubated with 5 mL of prewashed Dynabeads streptavidin M280 for 2 h at room temperature. The beads were washed 3 times with PBST (PBS at pH 7.4 with 0.1% Tween-20) and stored in PBS with 1% BSA at 4 °C until use.

Affinity capture of the target proteins from tissue samples was carried out on a KingFisher 96 magnetic particle processor (Thermo Electron). First, 20 μL of each antibody-coated bead (~2 μg of biotinylated antibody for each target for a total volume of 120 μL) was added to each well of a 96-deep-well plate (Thermo Fisher Scientific), and 80 μL of PBST was then added to reach a final volume of 200 μL. The mixed beads in each well were washed with 600 μL of PBST twice and were dispensed into another plate with 100 μg of human tissue lysate and mouse liver lysate containing calibration standards or QC samples in each well. The plate was then incubated for

DOI: 10.1021/acs.jproteome.8b00605
J. Proteome Res. 2018, 17, 3932−3940

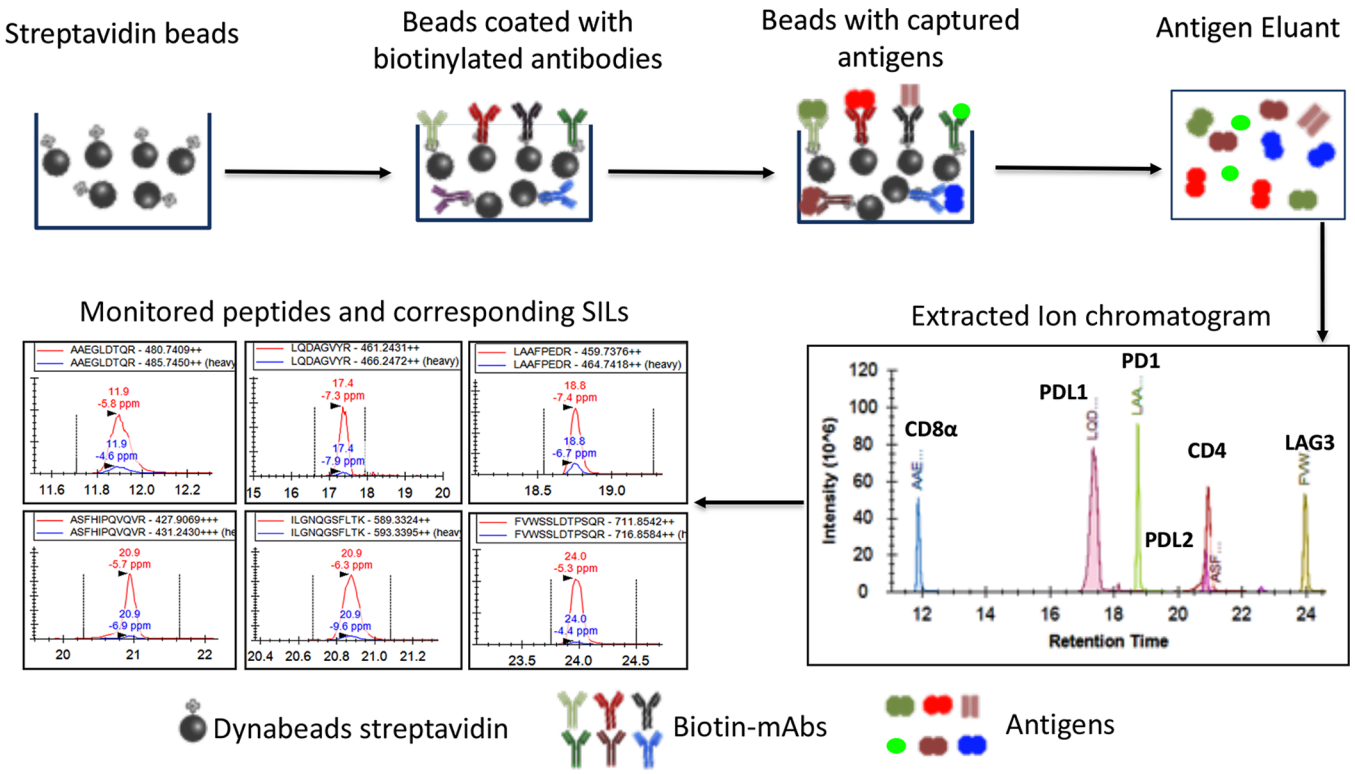

Figure 1. General assay workflow. Dynabeads coated with biotinylated antibodies against CD4, CD8A, LAG3, PD1, PD-L1, and PD-L1 were mixed and incubated with protein lysates extracted from frozen tissues. The antigens of interest were captured, eluted, denatured, and digested to generate a signature peptide from each protein. The corresponding stable-isotope-labeled peptides (SILs) were spiked into each sample as internal standards. Each processed sample was injected onto a pre-equilibated nano C18 trap column, and the peptides were separated by an easy nano C18 separation column followed by parallel reaction monitoring analysis using a Q Exactive Plus mass spectrometer.

4 h at room temperature followed by an overnight incubation at 4 °C. The beads with captured proteins were washed 3 times with 600 μL of HBS-EP (GE Healthcare), once with 600 μL of H_2O, and once with 600 μL of 10% acetonitrile in water. The target proteins were eluted by incubating the beads with 70 μL of 1% formic acid (FA) in 30% acetonitrile and 70% water for 15 min in a 96 well V-bottom elution plate. All of the samples in the plate were completely dried using SpeedVac.

Each sample was denatured and reduced in 20 μL of denaturing buffer (8 M urea, 10 mM TCEP in 0.1 M Tris at pH 8.0) for 1 h followed by alkylation with 5 mM of iodoacetamide (IAA) at room temperature for 30 min. Next, the digestion was performed using 15 ng of lys-C for 4 h followed by 1 μg of trypsin for 16 h at under 37 °C. The digestion was quenched by adding 5 μL of 10% FA. Heavy SIL peptides were freshly prepared at a final concentration of 0.2 nM in 0.1% FA and were 1:1 mixed with the digested peptides in a new 96 well V-bottom plate for LC–MS/MS analysis.

Liquid Chromatography and Mass Spectrometry

The digested peptides from each sample were trapped onto a nanoViper Acclaim PepMap100 C18 trap column (75 μm i.d. × 2 cm, 3 μm, 100 Å, Thermo) and then were separated by a nanoViper Acclaim PepMap RSLC C18 column (75 μm i.d. × 15 cm, 2 μm, 100 Å, Thermo) retrofitted with a SilcaTip (New Objective). A 55 min LC run was delivered by a M-class HPLC system (Waters Corporation) with mobile phase A (0.1% FA in H_2O) and B (0.1% FA in 100% acetonitrile) at 500 nL/min using the following gradient: 2% B for 12 min, 2–8% B in 1 min, 8% to 30% B in 24 min, 30%–80% B in 2 min, 80%–2% B in 2 min, and 2% B for 14 min. The trapping valve was switched to analytical flow at 8 min and switched back to trapping flow at 54 min. A detailed demonstration of switch valve setup was shown in Figure S9.

The eluted peptides of interest were analyzed by a Q Exactive Plus mass spectrometer (Thermo) in PRM mode. A full scan was acquired with the following settings: resolution of 70 000, AGC target of 3E6, max IT of 100 ms, and a scan range of 350–1500 m/z. For PRM, the settings were: resolution of 17 500, in-source CID of 0, AGC target of 2e5, max IT of 100 ms, loop count of 1, MSX count of 1, isolation window of 1.7 m/z, isolation offset of 0.0 m/z, and fixed first mass of 300 m/z. The inclusion list of peptides and the optimized NCE are listed in Table 1.

Data Processing

The abundance of each protein was calculated based on the peak area ratio of its endogenous peptide over the corresponding stable isotopic labeled peptide. The calibration curve of each protein was established by plotting the peak area ratio (Skyline Software) against protein concentration using a weighted ($1/x^2$) linear curve fit in PRISM software. The quality of the standard curves was evaluated by comparing the measured concentration of each calibration standard to its known concentration. The abundance of endogenous CD8A, CD4, LAG3, PD1, PD-L1, and PD-L2 in each tissue sample was calculated based on the calibration curves. The two-tailed Pearson Correlation was used to analyze the correlation between individual immune markers.

DOI: 10.1021/acs.jproteome.8b00605
J. Proteome Res. 2018, 17, 3932–3940

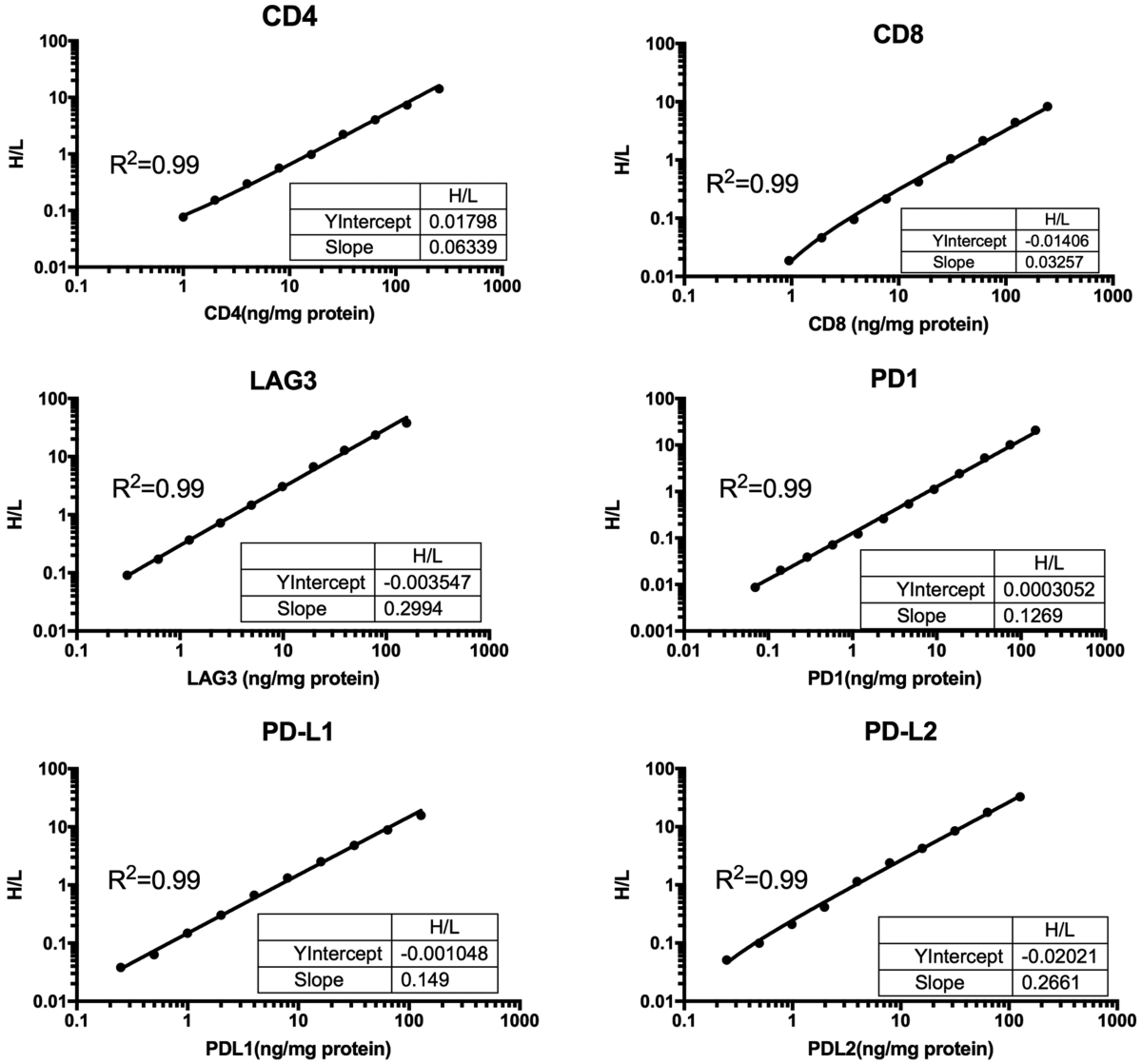

Figure 2. Representative assay validation calibration curves for all quantified immune markers. A total of 12 calibration standards of each protein were performed in every batch experiment. Linear regression weighted by $1/x2$ was applied to fit the curve.

Assay Validation

The assay was validated for accuracy, precision, limit of quantification, specificity, long-term stability, and system suitability. Calibration standards were tested on four different days with four repeats of QC samples at three different concentrations. The matrix only samples were also included to evaluate the specificity. The effect of using a surrogate matrix was evaluated by comparing the calculated concentration between mouse liver lysate and pooled human normal tissues spiked with different amount of target proteins. The long-term stability was assessed by storing QC samples and tumor lysates at −80 °C for 3 months. Variations in retention time and peak area of SILs were investigated to evaluate the system suitability. All parameters and acceptance criteria are listed in Table 1.

RESULTS AND DISCUSSION

A multiplex LC−MS/MS assay was designed and developed to accurately quantify the expression levels of CD8A, CD4, LAG3, PD1, PD-L1, and PD-L2 in normal and cancerous human tissues (Figure 1). The assay was optimized, automated and validated to provide a reliable and robust measurement of these biomarkers in frozen tissues.

Assay Development and Validation

Despite numerous studies that have applied LC−MS to quantify protein expression in tissues, the majority of them focused on antigens that are over-expressed by the tumor cells (HER2, ER, MET, etc.). The expression levels of MET in NSCLC ranged from 22 to 700 ng/mg total protein, while HER2 and ER expression ranged from 12 to 800 and 8−50 ng/mg in breast tissues, respectively. Compared with these studies, the quantitation of TILs markers requires higher sensitivity due to the low percentage of TILs in tumor and the low copy numbers of these markers.[16,17] Tryptic digests of recombinant CD8A, CD4, LAG3, PD1, PD-L1, and PD-L2 were first analyzed under the data-dependent acquisition mode. The two most-abundant tryptic peptides that uniquely presented in each protein (except for PD1, in which only one peptide passed the criteria) were selected from each protein after the removal of peptides with glycosylation site, methionine, and cysteine. Both peptides were monitored in the PRM assay, while one peptide that exhibited better sensitivity and reproducibility was used

DOI: 10.1021/acs.jproteome.8b00605
J. Proteome Res. 2018, 17, 3932−3940

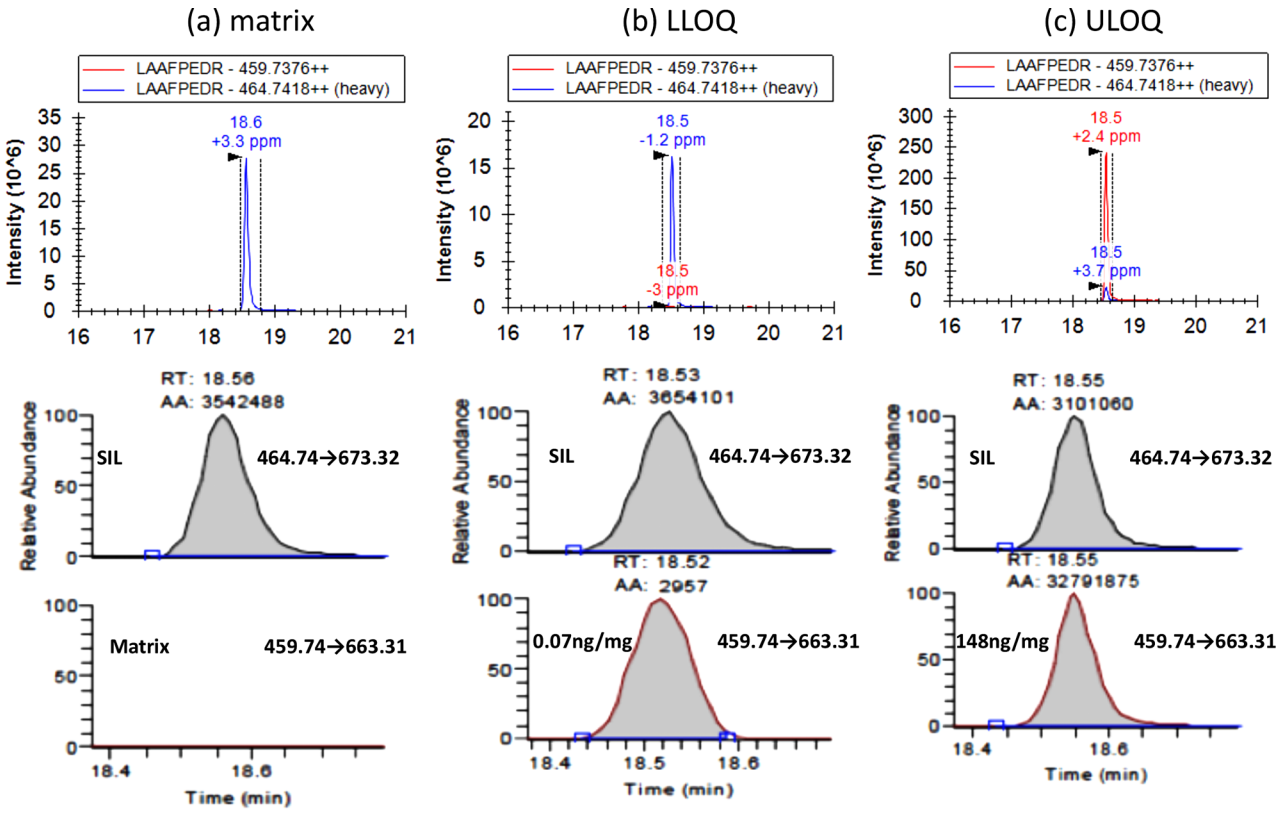

Figure 3. Extracted-ion chromatograms of monitored transitions for peptide LAAFPEDR and SIL of PD1 in (a) matrix, (b) LLOQ, and (c) ULOQ standards. The peptide was eluted at the same retention time (RT) for all three samples. The peak area of the SIL transition was similar, while the peak-area endogenous peptides were detected in a concentration-dependent manner. AA indicates the peak area.

Table 2. Summary of Assay Validation Statistics: Intra- and Interbatch Accuracy and Precision

	intrabatch	1	2	3	4	interbatch	1	2	3	4	interbatch	1	2	3	4	interbatch
target	*n*	4	4	4	4	4	4	4	4	4	4	4	4	4	4	4
		LQC (1.91 ng/mg total protein)					MQC (19.1 ng/mg total protein)					HQC (191 ng/mg total protein)				
CD4	mean	1.7	2	2.1	1.7	1.9	17	20.7	20.3	20.8	19.7	182.9	210.3	185	204.8	195.8
	CV (%)	3	7.7	6.7	5.7	11	3.4	4.3	5.7	9.9	9.2	6.5	9.1	14.7	7.3	7.1
	accuracy (%)	−13.4	2.7	10.7	−9.6	−2.4	−11	7.9	5.7	8.5	2.8	−4.6	9.7	−3.4	6.9	2.2
		LQC (1.84 ng/mg total protein)					MQC (18.4 ng/mg total protein)					HQC (184 ng/mg total protein)				
CD8A	mean	1.6	1.9	2	1.7	1.8	16.1	20.1	18.5	18.5	18.3	205.4	200.1	200.2	199.7	201.4
	CV (%)	11.4	7	1.7	6.8	10.1	7.6	4	4.6	5.1	9	10.9	8.7	5.1	4.7	1.3
	accuracy (%)	−11.2	1.7	7.1	−12.1	−3.6	−12	9.8	0.7	1	−0.1	11.9	9	9.1	8.8	9.7
		LQC (1.18 ng/mg total protein)					MQC (11.8 ng/mg total protein)					HQC (118 ng/mg total protein)				
LAG3	mean	1.2	1.3	1.1	1.2	1.2	12.7	10.7	12.5	12.9	12.2	131.9	136.2	115.8	125	127.2
	CV (%)	9.6	6	7.1	6.6	6.8	1.8	6.6	3.5	2.7	8.3	7.7	4.1	6.3	1.9	7
	accuracy (%)	2.1	13.1	−10.2	4.6	2.4	−7	−9.3	5.3	8.9	−0.5	11.3	15	−2.2	5.6	7.4
		LQC (1.11 ng/mg total protein)					MQC (11.1 ng/mg total protein)					HQC (111 ng/mg total protein)				
PD1	mean	1	1.3	1.1	1.3	1.2	9.6	12	11.4	12.9	11.5	103.4	115	114	125	114.4
	CV (%)	5.5	5.6	5.5	6.6	12.8	3.6	5.2	7.5	2.7	12.1	4.5	7.3	10.8	1.9	7.7
	accuracy (%)	−12.8	15	−2.1	4.6	1.2	−14	7.5	2.8	8.9	1.3	−7	3.3	2.5	5.6	1.1
		LQC (0.96 ng/mg total protein)					MQC (9.6 ng/mg total protein)					HQC (96.1 ng/mg total protein)				
PD-L1	mean	1	1	0.9	0.8	0.9	9.6	9.2	10.6	9.5	9.7	103.4	99.3	108.4	102	103.3
	CV (%)	5.5	4.6	4.5	3.1	10.4	3.6	4.9	3.7	4.2	6.2	2.5	0.8	5.5	1.9	3.7
	accuracy (%)	−12.8	1.7	−2.5	−11.4	−6.3	−14	−4.5	10.6	−1	−2.2	11.5	3.4	12.9	6.4	8.6
		LQC (0.95 ng/mg total protein)					MQC (9.5 ng/mg total protein)					HQC (95.0 ng/mg total protein)				
PD-L2	mean	1	0.9	0.9	1	1	8.4	8.6	10.6	10.6	9.6	79.1	86.2	95.4	104.2	91.2
	CV (%)	10.8	3.4	1.1	8.5	6.1	5.2	3	3.6	1.3	12.7	2	5.7	12.8	4.8	12
	accuracy (%)	1.7	−8	−4.2	−3.7	−3.6	−11.8	−8.9	11.4	11.6	0.6	−16.6	−9.2	0.6	9.9	−3.8

DOI: 10.1021/acs.jproteome.8b00605
J. Proteome Res. 2018, 17, 3932−3940

Table 3. Average Concentration and Standard Deviation of CD4, CD8A, LAG3, PD1, PD-L1, and PD-L2 and Total Protein Yields in Analyzed Tissue Samples[a]

protein (ng/mg)	LLOQ	liver (n = 4)	spleen(n = 4)	LNs(n = 4)	NAT(n = 4)	CT(n = 26)
CD4	1.00	3.02 ± 0.84	3.71 ± 0.61	10.59 ± 3.02	1.37 ± 0.45	4.32 ± 2.86
CD8A	0.95	1.27 ± 0.23 (n = 3)	8.82 ± 2.08	16.53 ± 1.95	1.51 ± 0.12 (n = 3)	10.17 ± 6.58
LAG3	0.15	BLQ	0.28 ± 0.15	0.45 ± 0.26 (n = 3)	BLQ	0.41 ± 0.24 (n = 17)
PD1	0.07	BLQ	BLQ	0.14 ± 0.01 (n = 2)	BLQ	0.12 ± 0.06 (n = 13)
PD-L1	0.25	0.27 ± 0.03	1.28 ± 0.39	1.10 ± 0.47	BLQ	1.45 ± 1.16 (n = 22)
PD-L2	0.25	BLQ	BLQ	0.57 ± 0.27 (n = 2)	0.34 (n = 1)	0.32 ± 0.08 (n = 9)
protein yield (%)		12.48 ± 1.01	10.03 ± 1.35	5.95 ± 1.35	4.82 ± 1.43	8.47 ± 2.11

[a]LLOQ refers to the lower limit of quantitation. Samples that had target expression levels lower than LLOQ were excluded from the calculation of average concentration; n refers to the number of samples used for quantitation; BLQ indicates that all of the samples in the tested group had target expressions below LLOQ.

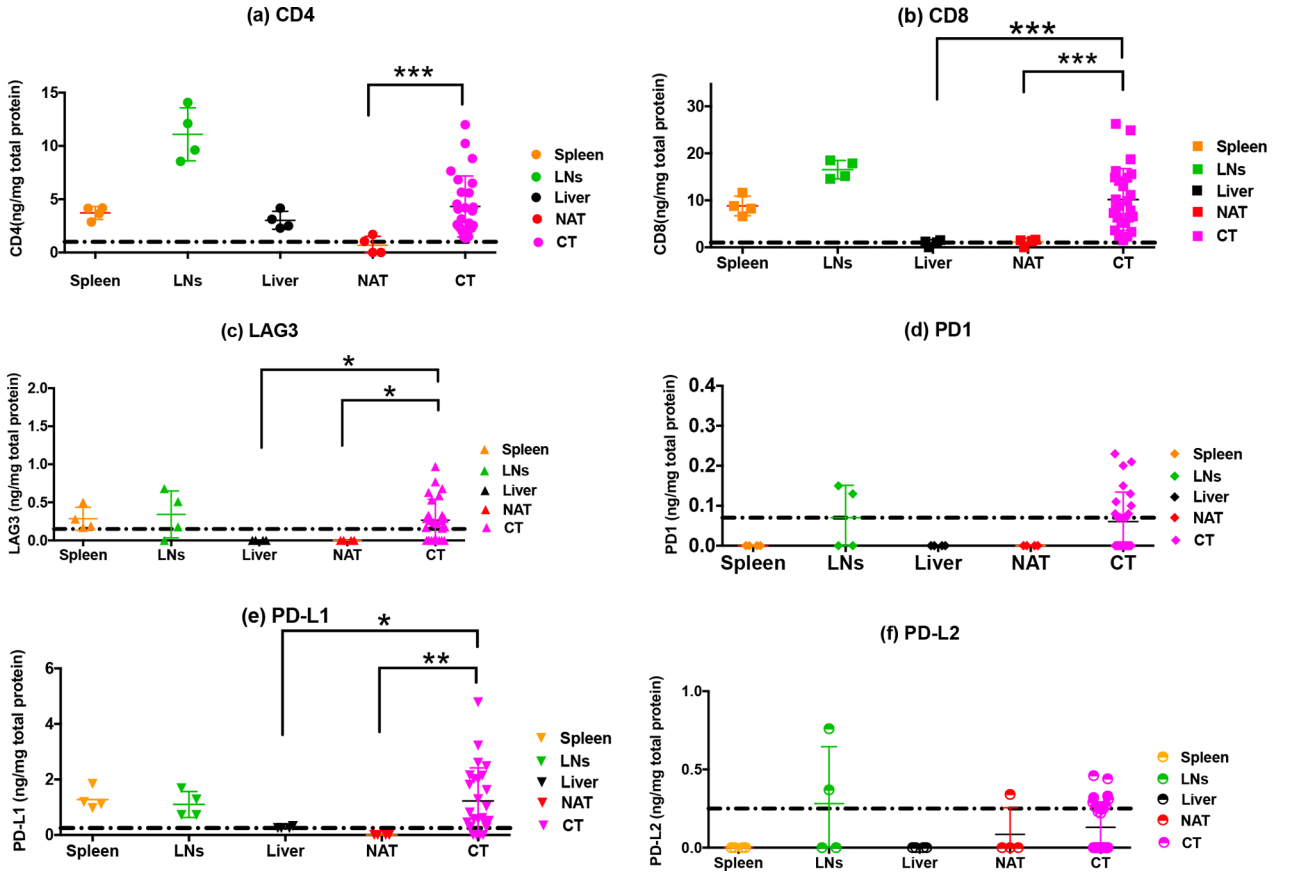

Figure 4. Expression of CD4, CD8A, LAG3, PD1, PD-L1, and PD-L2 in human liver, spleen, cervical lymph nodes (LNs), normal adjacent tissues (NAT), and cervical tumors (CT). Significantly higher expression of CD4, CD8, LAG3, PD1, and PD-L1 were detected in the CT group compared to the NAT group (single asterisks indicate $p < 0.05$, double asterisks indicate $p < 0.01$, and triple asterisks indicate $p < 0.001$ calculated by Mann–Whitney test). The LLOQ of each protein is indicated with a dashed line. Samples that had target expression levels below LLOQ were replaced.

for the quantitation and validation. Using automated affinity enrichment and optimized sample preparation procedures, we were able to achieve LLOQs from 0.07 to 1 ng/mg (Table1), values that are ∼10−100 fold lower than most previous reports. The LC gradient was optimized to reach the lowest LLOQ for PD1 (0.07 ng/mg) and the second lowest for LAG3 (0.15 ng/mg). LLOQ was defined as the lowest concentration of calibration standards with accuracy within 25% for all 4 replicated experiments. The LLOQs of PD-L1, PD-L2, CD4, and CD8A were 0.25, 0.25, 1.00, and 0.95 ng/mg, respectively. LLODs of these proteins were points (1/2 or 1/4) lower than LLOQ with batch-to-batch variation observed. The sensitivity of our assay was similar to the sensitivity reported by Morales-Betanzos et al., in which an offline basic reverse-phase LC separation coupled with nano-LC−PRM was used to quantify the levels of PD1, PD-L1, and PD-L2 in melanoma tissues.[18] While additional separation would significantly improve assay sensitivity, it is not ideal for high-throughput quantitation of multiple proteins. In our case, all 6 proteins were quantified simultaneously within a 1 h nanoflow LC run with excellent reproducibility. Minimal variation in retention time was observed, with an intrabatch variation of 0.04−0.37 min and an interbatch variation of 0.10−0.75 min (Table S8 and Figure S8).

Once developed, the assay was assessed for accuracy, precision, selectivity, matrix effect, and stability. Validation

DOI: 10.1021/acs.jproteome.8b00605
J. Proteome Res. 2018, 17, 3932−3940

parameters and acceptance criteria can be found in the Supporting Information. A total of four replicates of validation samples at three different concentrations were measured across four different batches to assess the intra- and interassay precision and accuracy. All batches passed the validation and the summarized results are listed in Table S1. Representative calibration curves for all proteins are shown in Figure 2, and excellent linearity was observed from all batches (Figure S1). The extracted-ion chromatograms (XICs) of PD1 peptides and the corresponding SIL peptides for matrix blank as well as matrix spiked with PD1 at the LLOQ and ULOQ levels are shown in Figure 3. The XICs of other signature peptides from CD4, CD8A, LAG3, PD-L1, and PD-L2 are shown in Figures S2, S3, S4, S5, and S6, respectively. Minimal background was detected for all monitored transitions in matrix blanks (pooled mouse liver lysates).

As shown in Table 2, good precision and accuracy were achieved. The intrabatch accuracy ranged within −16.6% to 15.0% for all proteins at all concentrations, and the precision ranged from 0.8% to 14.7%, while interbatch accuracy ranged within −6.3% to 8.6% and the precision ranged from 1.3% to 12.8%. The measured concentrations of all calibration standards and QCs from all batches were listed in Tables S2, S3, S4, S5, S6, and S7, respectively. Long-term stability was also evaluated by comparing the concentrations of QC standards and 26 tumor samples before and after 3 months of storage at −80 °C. The variation ranged from 0.7 to 12.9% for QC standards prepared in mouse liver lysate, and the variation ranged from 4.3 to 12.0% for individual tumor lysates from human cervical tumors, indicating that the assay can be used for long-term stored samples.

The variations in measured concentrations of LAG3, PD1, PD-L1, and PD-L2 between mouse liver lysate and non-tumor human skin tissue adjacent to malignant melanoma (normal adjacent tissue; NAT) were all below 25%. For CD4 and CD8A, higher concentrations were detected in NAT matrix at spike-in concentrations of 1.00 and 2.00 ng/mg due to the endogenous expression or blood contamination of CD4 and CD8A in human tissues (Table S8). The intensities of all SIL peptides from the same batch had variations below 25% across calibration standards and tested tumor samples, confirming that different matrices had minimal assay interferences (Figure S7).

Quantitation of CD8A, CD4, LAG3, PD1, PD-L1, and PD-L2 in Human Tissue Samples

The validated assay was then utilized to quantify the expression of CD8A, CD4, LAG3, PD1, PD-L1, and PD-L2 in human liver (n = 4), spleen (n = 4), and cervical lymph nodes (LNs, n = 4) from nontumor human tissues, normal skin tissue adjacent to malignant melanoma (n = 4), and cervical tumors (CT, n = 26). Cervical cancer was selected as a tumor type with moderate-to-low immune infiltration and response to checkpoint inhibitor therapy.[19] The results are summarized in Table 3.

High concentrations of CD8A (16.52 ng/mg) and CD4 (10.59 ng/mg) were detected in lymph nodes, and moderate expression of CD8A (8.82 ng/mg) and CD4 (3.72 ng/mg) was detected in spleen, another lymphoid organ, while a low level of CD8A (1.27 ng/mg) and medium expression of CD4 (3.02 ng/mg) were detected in liver, a nonlymphoid organ. This is the first report in which absolute levels of CD8A and CD4 were quantified in tissues. Our results agree well with the observation by Katrin et al. of a similar distribution of total lymphocytes in lymph nodes (190 × 10^9), spleen (70× 10^9), and liver (10× 10^9).[20] Significantly higher expression levels of CD8A were detected in tissues from cervical tumor compared with NAT and liver (Figure 4b). The average expression levels of CD8A in 26 cervical tumors (10.17 ± 6.58 ng/mg) were comparable to those of lymph nodes (16.52 ± 1.95 ng/mg), confirming the prevalence of tumor infiltrating T cells. Interestingly, a wide dynamic range in CD8A expression (1.49−26.27 ng/mg) was observed in different cervical tumors, which is consistent with the heterogeneous presence of these cells in tumors reported by numerous IHC studies and the requirement for PD-L1 testing prior to the administration of anti-PD1 therapy.

Half of cervical tumors (13 of 26) showed detectable levels of PD1 ranging from 0.07 to 0.23 ng/mg total protein (Figure 4d). PD-L1 and PD-L2, which are known ligands of PD1, were detected in 85% (1.45 ± 1.16 ng/mg) and 35% (0.32 ± 0.08 ng/mg) of cases, respectively (Figure 4e,f). Although PD-L2 was only detected in 9 of 26 tumors, a strong correlation (r^2 = 0.79, p < 0.01) between PD-L1 and PD-L2 was observed. Surprisingly, the expression of PD1 did not correlate with PD-L1 or PD-L2, possibly because PD1 is expressed at a relatively low level close to the LLOQ with a narrow expression range (0.07−0.23 ng/mg). Among the 3 proteins, PD-L1 had the highest concentration in the tested tumors. In an analysis of PD-L1 expression in 93 cervical carcinoma tissues by IHC, positive PD-L1 expression was reported in 73.1% of cases, suggesting that our LC−MS assay has comparable sensitivity in detecting PD-L1.[21]

LAG3, another important inhibitory receptor expressed on T cells, was detected in 75% (17 of 26) of cervical tumors at levels ranging from 0.17 to 0.97 ng/mg total protein. Because the LC−PRM assay enabled the simultaneous quantitation of all six markers, it affords the opportunity to investigate the correlation between the different immune markers in the absence of experimental variation from sampling and processing. Despite the limited number of cervical tumor samples analyzed, a correlation was observed between LAG3 and CD4 (r^2 = 0.85), CD8A (r^2 = 0.86), PD-L1 (r^2 = 0.86), and PD-L2 (r^2 = 0.74) (Table 4 and Figure 5). Numerous studies have investigated the synergistic effects of LAG3/MHCII and PD1/PD-L1 pathways in regulating T-cell activity.[22] Our results provided experimental evidence implicating both pathways in the microenvironment of cervical cancer.

Table 4. Correlation between Quantified Immune Markers in 26 Cervical Tumors[a]

correlation (r)	CD4	CD8a	LAG3	PD1	PD-L1	PD-L2
CD4	1.00					
CD8A	0.88[c]	1.00				
LAG3	0.77[c]	0.86[c]	1.00			
PD1	0.33	0.18	0.12	1.00		
PD-L1	0.51[b]	0.64[c]	0.81[c]	0.02	1.00	
PD-L2	0.56[b]	0.54[b]	0.73[c]	0.25	0.79[b]	1.00

[a]A two-tailed Pearson correlation was used to analyze the correlation between individual immune markers. [b]p < 0.01. [c]p < 0.001.

DOI: 10.1021/acs.jproteome.8b00605
J. Proteome Res. 2018, 17, 3932−3940

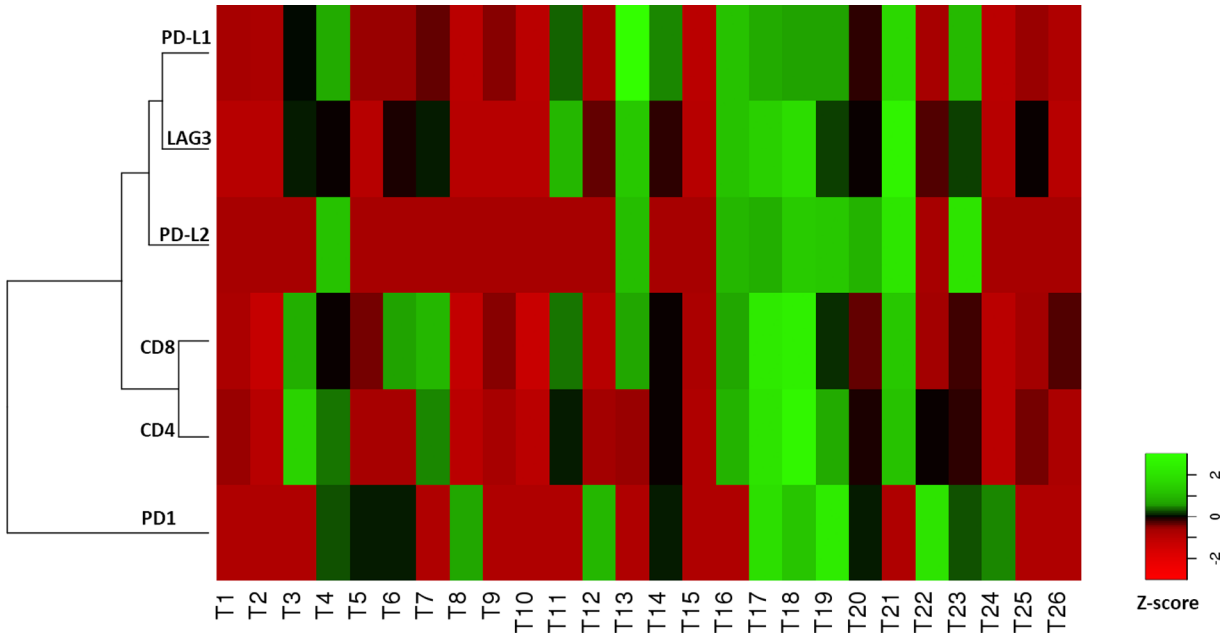

Figure 5. Heat-map and cluster analysis of expression for CD4, CD8A, LAG3, PD-L1, and PD-L2 in cervical tumors (n = 26). Expression levels of each protein were normalized to the z-score presented by the color plot. The red to green color represents the value of protein expression from low to high in analyzed tumor samples. The strongest correlations were observed between CD4 and CD8 then PD-L1.

Assay Considerations

A multiplexed LC−MS−PRM assay was developed to quantify the expression of immune biomarkers in frozen tissues. Variation in protein extraction was observed across different types of tissues (Tables 3 and Table S11). The CV in protein extraction yield was within 25% for the same tissue type, while a significantly smaller amount of protein was extracted from LNs and NATs compared with liver, spleen, and cervical tumors. This would not affect the target quantitation or comparisons within the same tissue type but will need to be considered when comparing target distribution across different tissues. Although the PRM assay may provide improved accuracy and consistency by simultaneously quantifying multiple biomarkers at the protein level, it fails to retain the spatial information of these markers in individual cells as IHC does. The development and validation of this assay provides a complementary approach to IHC for target quantitation in clinical tissue samples. Future studies could cross-compare results obtained with LC−MS−PRM, IHC, RNA-Seq, RNA-Scope, and other methods as well as correlations with clinical outcomes.

CONCLUSIONS

We developed a novel immunoaffinity-based LCS−PRM assay for simultaneous quantitation of immune markers CD8A, CD4, LAG3, PD1, PD-L1, and PD-L2 from frozen tissues. The superior sensitivity and robustness of this assay allows the accurate quantification of all six immune markers and provides the advantage of investigating their correlations with no variation in sample processing. Through the implementation of automated sample preparation and optimized LC separation, we successfully validated the assay and applied it to analyze the expression of these immune makers in different tissue sources. Significant correlation was observed between LAG3, CD4, CD8A, PD-L1, and PD-L2 in 26 cervical tumors, suggesting that these markers provide independent measures of the inflammatory state of the tumors. LC−PRM offers several potential advantages over conventional IHC methods that include multiplexing capability, quantitative ability, reproducibility and specificity. It could also be combined with IHC or an RNA scope to obtain comprehensive information on both spatial and expression relationships of immune-checkpoint proteins. To our knowledge, this is the first validated immuno-LC−PRM assay that quantifies multiple immune targets in clinical tissue samples.

ASSOCIATED CONTENT

Supporting Information

The Supporting Information is available free of charge on the ACS Publications website at DOI: 10.1021/acs.jproteome.8b00605.

Assay validation parameters, acceptance criteria, assay results measured concentrations; tables showing a summary of validation results; the characterization and quantitation of the immune markers, calibration standards in different matrices, long-term storage effects, the retention time of all monitored peptides, sample information for 26 cervical tumors, and overall peptides monitored in the LC−MS experiment; figure showing standard curves, extracted ion chromatograms, peak areas of SIL peptides in different matrices, the retention time of monitored signature peptides and corresponding SILs, and the switch valve setup of the M-class LC system (PDF)

AUTHOR INFORMATION

Corresponding Author

*E-mail: ylyashuliu@gmail.com.

ORCID

Yashu Liu: 0000-0002-5707-4823

DOI: 10.1021/acs.jproteome.8b00605
J. Proteome Res. 2018, 17, 3932−3940

Notes

The authors declare no competing financial interest.
The raw mass spec spectrometry data from a complete set of studies can be found on ProteomeXchange under the project name "Multiplex PRM quantitation of CD8a, CD4, LAG3, PD1, PD-L1 and PD-L2" with project accession code PXD011152.

■ ABBREVIATIONS

LAG3, lymphocyte activation gene-3; PD1, program death protein 1; PD-L1, program death protein ligand 1; PD-L2, program death protein ligand 2; TIL, tumor infiltrating lymphocytes; HQC, high concentration of quality control; MQC, medium concentration of quality control; LQC, low concentration of quality control; TILs, tumor-infiltrating lymphocytes; PRM, parallel reaction monitoring

■ REFERENCES

(1) Boon, T.; Coulie, P. G.; Van den Eynde, B. J.; van der Bruggen, P. Human T cell responses against melanoma. *Annu. Rev. Immunol.* **2006**, *24*, 175−208.

(2) Chikuma, S.; Terawaki, S.; Hayashi, T.; Nabeshima, R.; Yoshida, T.; Shibayama, S.; Okazaki, T.; Honjo, T. PD1-mediated suppression of IL-2 production induces CD8+ T cell anergy in vivo. *J. Immunol.* **2009**, *182* (11), 6682−9.

(3) Huang, C. T.; Workman, C. J.; Flies, D.; Pan, X.; Marson, A. L.; Zhou, G.; Hipkiss, E. L.; Ravi, S.; Kowalski, J.; Levitsky, H. I.; Powell, J. D.; Pardoll, D. M.; Drake, C. G.; Vignali, D. A. Role of LAG-3 in regulatory T cells. *Immunity* **2004**, *21* (4), 503−13.

(4) Bellmunt, J.; de Wit, R.; Vaughn, D. J.; Fradet, Y.; Lee, J. L.; Fong, L.; Vogelzang, N. J.; Climent, M. A.; Petrylak, D. P.; Choueiri, T. K.; Necchi, A.; Gerritsen, W.; Gurney, H.; Quinn, D. I.; Culine, S.; Sternberg, C. N.; Mai, Y.; Poehlein, C. H.; Perini, R. F.; Bajorin, D. F. Pembrolizumab as Second-Line Therapy for Advanced Urothelial Carcinoma. *N. Engl. J. Med.* **2017**, *376* (11), 1015−1026.

(5) Gandhi, L.; Rodriguez-Abreu, D.; Gadgeel, S.; Esteban, E.; Felip, E.; De Angelis, F.; Domine, M.; Clingan, P.; Hochmair, M. J.; Powell, S. F.; Cheng, S. Y.; Bischoff, H. G.; Peled, N.; Grossi, F.; Jennens, R. R.; Reck, M.; Hui, R.; Garon, E. B.; Boyer, M.; Rubio-Viqueira, B.; Novello, S.; Kurata, T.; Gray, J. E.; Vida, J.; Wei, Z.; Yang, J.; Raftopoulos, H.; Pietanza, M. C.; Garassino, M. C.; Investigators, K.-. Pembrolizumab plus Chemotherapy in Metastatic Non-Small-Cell Lung Cancer. *N Engl J. Med.* **2018**, *378* (22), 2078−2092.

(6) Borghaei, H.; Paz-Ares, L.; Horn, L.; Spigel, D. R.; Steins, M.; Ready, N. E.; Chow, L. Q.; Vokes, E. E.; Felip, E.; Holgado, E.; Barlesi, F.; Kohlhaufl, M.; Arrieta, O.; Burgio, M. A.; Fayette, J.; Lena, H.; Poddubskaya, E.; Gerber, D. E.; Gettinger, S. N.; Rudin, C. M.; Rizvi, N.; Crino, L.; Blumenschein, G. R.; Antonia, S. J.; Dorange, C.; Harbison, C. T.; Graf Finckenstein, F.; Brahmer, J. R. Nivolumab versus Docetaxel in Advanced Nonsquamous Non-Small-Cell Lung Cancer. *N. Engl. J. Med.* **2015**, *373* (17), 1627−39.

(7) Socinski, M. A.; Jotte, R. M.; Cappuzzo, F.; Orlandi, F.; Stroyakovskiy, D.; Nogami, N.; Rodriguez-Abreu, D.; Moro-Sibilot, D.; Thomas, C. A.; Barlesi, F.; Finley, G.; Kelsch, C.; Lee, A.; Coleman, S.; Deng, Y.; Shen, Y.; Kowanetz, M.; Lopez-Chavez, A.; Sandler, A.; Reck, M. Atezolizumab for First-Line Treatment of Metastatic Nonsquamous NSCLC. *N. Engl. J. Med.* **2018**, *378* (24), 2288−2301.

(8) Powles, T.; Duran, I.; van der Heijden, M. S.; Loriot, Y.; Vogelzang, N. J.; De Giorgi, U.; Oudard, S.; Retz, M. M.; Castellano, D.; Bamias, A.; Flechon, A.; Gravis, G.; Hussain, S.; Takano, T.; Leng, N.; Kadel, E. E., 3rd; Banchereau, R.; Hegde, P. S.; Mariathasan, S.; Cui, N.; Shen, X.; Derleth, C. L.; Green, M. C.; Ravaud, A. Atezolizumab versus chemotherapy in patients with platinum-treated locally advanced or metastatic urothelial carcinoma (IMvigor211): a multicentre, open-label, phase 3 randomised controlled trial. *Lancet* **2018**, *391* (10122), 748−757.

(9) Zhang, Q.; Spellman, D. S.; Song, Y.; Choi, B.; Hatcher, N. G.; Tomazela, D.; Beaumont, M.; Tabrizifard, M.; Prabhavalkar, D.; Seghezzi, W.; Harrelson, J.; Bateman, K. P. Generic automated method for liquid chromatography-multiple reaction monitoring mass spectrometry based monoclonal antibody quantitation for preclinical pharmacokinetic studies. *Anal. Chem.* **2014**, *86* (17), 8776−84.

(10) Neubert, H.; Muirhead, D.; Kabir, M.; Grace, C.; Cleton, A.; Arends, R. Sequential protein and peptide immunoaffinity capture for mass spectrometry-based quantification of total human beta-nerve growth factor. *Anal. Chem.* **2013**, *85* (3), 1719−26.

(11) Kennedy, J. J.; Whiteaker, J. R.; Schoenherr, R. M.; Yan, P.; Allison, K.; Shipley, M.; Lerch, M.; Hoofnagle, A. N.; Baird, G. S.; Paulovich, A. G. Optimized Protocol for Quantitative Multiple Reaction Monitoring-Based Proteomic Analysis of Formalin-Fixed, Paraffin-Embedded Tissues. *J. Proteome Res.* **2016**, *15* (8), 2717−28.

(12) Narumi, R.; Shimizu, Y.; Ukai-Tadenuma, M.; Ode, K. L.; Kanda, G. N.; Shinohara, Y.; Sato, A.; Matsumoto, K.; Ueda, H. R. Mass spectrometry-based absolute quantification reveals rhythmic variation of mouse circadian clock proteins. *Proc. Natl. Acad. Sci. U. S. A.* **2016**, *113* (24), E3461.

(13) He, J.; Sun, X.; Shi, T.; Schepmoes, A. A.; Fillmore, T. L.; Petyuk, V. A.; Xie, F.; Zhao, R.; Gritsenko, M. A.; Yang, F.; Kitabayashi, N.; Chae, S. S.; Rubin, M. A.; Siddiqui, J.; Wei, J. T.; Chinnaiyan, A. M.; Qian, W. J.; Smith, R. D.; Kagan, J.; Srivastava, S.; Rodland, K. D.; Liu, T.; Camp, D. G., 2nd Antibody-independent targeted quantification of TMPRSS2-ERG fusion protein products in prostate cancer. *Mol. Oncol.* **2014**, *8* (7), 1169−80.

(14) Laiho, J. E.; Oikarinen, M.; Richardson, S. J.; Frisk, G.; Nyalwidhe, J.; Burch, T. C.; Morris, M. A.; Oikarinen, S.; Pugliese, A.; Dotta, F.; Campbell-Thompson, M.; Nadler, J.; Morgan, N. G.; Hyoty, H. Relative sensitivity of immunohistochemistry, multiple reaction monitoring mass spectrometry, in situ hybridization and PCR to detect Coxsackievirus B1 in A549 cells. *J. Clin. Virol.* **2016**, *77*, 21−8.

(15) Sprung, R. W.; Martinez, M. A.; Carpenter, K. L.; Ham, A. J.; Washington, M. K.; Arteaga, C. L.; Sanders, M. E.; Liebler, D. C. Precision of multiple reaction monitoring mass spectrometry analysis of formalin-fixed, paraffin-embedded tissue. *J. Proteome Res.* **2012**, *11* (6), 3498−505.

(16) Pruneri, G.; Gray, K. P.; Vingiani, A.; Viale, G.; Curigliano, G.; Criscitiello, C.; Lang, I.; Ruhstaller, T.; Gianni, L.; Goldhirsch, A.; Kammler, R.; Price, K. N.; Cancello, G.; Munzone, E.; Gelber, R. D.; Regan, M. M.; Colleoni, M. Tumor-infiltrating lymphocytes (TILs) are a powerful prognostic marker in patients with triple-negative breast cancer enrolled in the IBCSG phase III randomized clinical trial 22−00. *Breast Cancer Res. Treat.* **2016**, *158* (2), 323−31.

(17) Inoue, Y.; Yoshimura, K.; Mori, K.; Kurabe, N.; Kahyo, T.; Mori, H.; Kawase, A.; Tanahashi, M.; Ogawa, H.; Inui, N.; Funai, K.; Shinmura, K.; Niwa, H.; Suda, T.; Sugimura, H. Clinical significance of PD-L1 and PD-L2 copy number gains in non-small-cell lung cancer. *Oncotarget* **2016**, *7* (22), 32113−28.

(18) Morales-Betanzos, C. A.; Lee, H.; Gonzalez Ericsson, P. I.; Balko, J. M.; Johnson, D. B.; Zimmerman, L. J.; Liebler, D. C. Quantitative Mass Spectrometry Analysis of PD-L1 Protein Expression, N-glycosylation and Expression Stoichiometry with PD1 and PD-L2 in Human Melanoma. *Mol. Cell. Proteomics* **2017**, *16* (10), 1705−1717.

(19) Pembrolizumab OK'd for Cervical Cancer. *Cancer Discovery* **2018**.8904

(20) Blum, K. S.; Pabst, R. Lymphocyte numbers and subsets in the human blood. Do they mirror the situation in all organs? *Immunol. Lett.* **2007**, *108* (1), 45−51.

(21) Reddy, O. L.; Shintaku, P. I.; Moatamed, N. A. Programmed death-ligand 1 (PD-L1) is expressed in a significant number of the uterine cervical carcinomas. *Diagn. Pathol.* **2017**, *12* (1), 45.

(22) Nguyen, L. T.; Ohashi, P. S. Clinical blockade of PD1 and LAG3–potential mechanisms of action. *Nat. Rev. Immunol.* **2015**, *15* (1), 45−56.

DOI: 10.1021/acs.jproteome.8b00605
J. Proteome Res. 2018, 17, 3932−3940